Ab Initio Study of the Hydroxylated Surface of Amorphous Silica: A Representative Model

Frederik Tielens,*,† Christel Gervais,‡ Jean François Lambert,† Francesco Mauri,§ and Dominique Costa||

Laboratoire de Réactivité de Surface and Laboratoire de Chimie de la Matière Condensée, Université Pierre et Marie Curie-Paris6, 4, Place Jussieu, F-75252 Paris Cedex 05, France, Institut de Minéralogie et Physique des Milieux Condensés, Université Pierre et Marie Curie-Paris6, Campus Boucicaut, 140 rue de Lourmel, 75015 Paris, France, and Laboratoire de Physico-Chimie des Surfaces, Ecole Nationale Supérieure de Chimie de Paris, 11 rue Pierre et Marie Curie, F-75231 Paris cedex, France

Received January 11, 2008. Revised Manuscript Received March 4, 2008

A new complete, representative model for the hydroxylated surface of amorphous silica is presented and characterized by means of periodic DFT calculations. This model accounts for the experimentally encountered ring size distribution, Si−O−Si and O−Si−O angles, silanols density, and distribution (isolated, associated, geminals). Properties such as NMR shifts, dehydrogenation energies, OH vibrational frequencies, and the interaction with water are investigated. The results are compared with former experimental and theoretical results. This new representative model for this complex surface would probably help the investigation of its reactivity toward amino acids or other organic molecules, opening new perspectives in the understanding of the chemistry of amorphous materials.

Introduction

Silica, the most common mineral on Earth, is used for applications in catalysis and chromatography and is a key component in electronic devices, solar cells, and optical fibers.[1] Its chemical properties have been widely studied and reviewed.[2,3] Silica polymorphs are composed of SiO_4 tetrahedra which polymerize forming different structures. The flexibility of the Si−O−Si bond explains the great number of existing polymorphs, either natural or synthetic: several crystalline forms such as quartz, cristobalite, tridymite, diatomite, and edingtonite, a number of noncrystalline glasses or sol−gel phases, and micro/mesoporous materials.

When created by cleavage, the silica surface exhibits undercoordinated atoms such as three coordinated Si atoms, terminal (nonbridging) oxygens, and strained Si−O−Si bridges in small size rings. The silica defects readily react with water in ambient conditions to form surface hydroxyl groups named silanols[3–6] which can make the surface hydrophilic (vide infra). In contrast, a nondefective surface is hydrophobic.[7–10]

Due to the noncrystalline nature of silica, the classical diffraction techniques cannot be used to give structural information. Yet its surface seems to exhibit a quite rich diversity of chemical groups.

The first important distinction that must be made here is between the terminal and geminal silanols. Terminal silanols are bound to a Si atom involved in three Si−O−Si siloxane groups, whereas geminal silanols complete the coordination sphere of a Si atom involved in two siloxane groups. Sometimes, longer-range interactions are taken into account: two silanols on Si atoms connected by a siloxane bridge are vicinal; they are adjacent if the Si atoms are separated by an O−Si−O bridge. A terminal silanol could be engaged in either vicinal or adjacent relations, both, or neither, and the same holds for a silanol in a geminal pair.

In addition to this distinction based on through-bond interactions, silanols may differ according to through-space neighboring relations: they may be H bonded to other silanols (in which case they are said to be associated) or not: they are then isolated.

The methods available to characterize silica surfaces give information on either of these distinctions. The silanols on the surface of amorphous silica have been characterized

* Author to whom correspondence should be sent. E-mail: tielens@ccr.jussieu.fr.
† Laboratoire de Réactivité de Surface, Université Pierre et Marie Curie-Paris6.
‡ Laboratoire de Chimie de la Matière Condensée, Université Pierre et Marie Curie-Paris6.
§ Institut de Minéralogie et Physique des Milieux Condensés, Université Pierre et Marie Curie-Paris6.
|| Ecole Nationale Supérieure de Chimie de Paris.

(1) Bakos, T.; Rashkeev, S. N.; Pantelides, S. T. *Phys. Rev. Lett.* **2002**, *88*, 055508.
(2) Legrand, A. P. *The Surface Properties of Silicas*; Wiley: New York, 1998.
(3) Iler, R. K. *The Chemistry of Silicas*; Wiley: New York, 1979.
(4) KnozingerH. *The Hydrogen Bond*; North Holland: Amsterdam, 1976; Vol. 3.
(5) Zhuravlev, L. T. *Langmuir* **1987**, *3*, 316.
(6) Nishijima, M.; Edamoto, K.; Kubota, Y.; Tanaka, S.; Onchi, M. *J. Phys. Chem.* **1986**, *84*, 6458.
(7) Bolis, V.; Fubini, B.; Marchese, L.; Martra, G.; Costa, D. *J. Chem. Soc., Faraday Trans.* **1991**, *87*, 497.
(8) Sindorf, D. W.; Maciel, G. E. *J. Am. Chem. Soc.* **1983**, *105*, 1487.
(9) D'Souza, A. S.; Pantano, C. G. *J. Am. Ceram. Soc.* **2002**, *85*, 1499.
(10) Wendt, S.; Frerichs, M.; Wei, T.; Chen, M. S.; Kempter, V.; Goodman, D. W. *Surf. Sci.* **2004**, *565*, 107.

10.1021/cm8001173 CCC: $40.75
Published on Web 04/25/2008

mainly by means of IR[11,12] and Raman[13,14] as well as ^{29}Si MAS and CP-MAS[8,15–18] and ^{1}H MAS[19–26] NMR.

Vibrational spectroscopies mostly respond to the degree of association of the silanol groups. The OH stretching frequencies of associated silanols are observed in a broadband centered on 3550 cm^{-1}, while isolated silanols vibrate at 3747−3750 cm^{-1}. [2,3,27,28]

^{29}Si NMR provides information on the state of covalent binding (geminal or terminal) of the silanol groups: geminal silanols correspond to "Q^2" environments for the silicon atom, whose nucleus resonates at about −90 ppm, and terminal silanols to "Q^3" environments for the silicon, resonating around −100 ppm. Recently, methods were proposed to perform the quantification of protons by ^{1}H MAS NMR in silicas.[29,30]

Besides providing an independent estimate of the total density of silanols, they allowed discrimination between associated, accessible isolated, and inaccessible isolated silanols. The insulator nature of silica compromises the use of classical surface tools because of sample charging effects. X-ray photoelectron spectroscopy has been scarcely used[31,32] for surface site characterization, although thin SiO_2 films may be synthesized to overcome this technical limit, and some studies on the reactivity of amorphous thin films of SiO_2 on Si(100) and Si(111) were performed.[6,33] Freund's group synthesized a flat and homogeneous monocrystalline SiO_2 layer on Mo(112),[34,35] which was used later on by Goodman et al. and others.[10,36,37]

A representative model of the silica surface should reproduce what is known about the silanol density and the distribution among the various kinds of silanols. Some precipitated silicas can expose as many as 7 OH/nm^2,[27] but in most studies the average reported density is 4.9 ± 1 OH/nm^2,[5] as compared to a total of 8 surface Si atoms/nm^2.[38]

The measured proportion of geminal silanols is more uncertain and depends on the type of silica as well as on the degree of humidity of the atmosphere. Indeed, geminal silanols are expected to be stabilized in the presence of water (vapor or liquid). Various authors have reported that geminal silanols amount to 9−30% of the total silanol population on amorphous silica.[18,39,40] A quite typical value of 14% geminal silanols was obtained for an Aerosil-type silica by ^{29}Si NMR.[41]

Other claims are quite different. Using the technique of evanescent wave cavity ringdown spectroscopy, Fisk et al.[42] have reported that the surface of a quartz prism in contact with a water solution exhibited two silanols with different acidities (pK_a), in the relative proportions of 27% (more acidic) to 73% (less acidic). They assigned the first group to terminal and the second to geminal silanols: that is, the geminal Si-OH would then constitute a 3/4 majority. However, the basis for this assignment is unclear. Even if it is justified, the substrate under study was quite different from amorphous silica.

In an SFG (sum frequency generation) study of a silica prism in contact with solutions of variable pH, Ong et al. also distinguished two surface groups of different acidities, with 15−20% of the more acidic one and 80−85% of the other, but they refrained from a precise assignment of both groups.[43] Thus, based on currently available evidence, we believe that a representative model of silica should include a minority of geminal silanols in the 10−30% range.

The silanols are responsible for the silica reactivity. Among other studied probes, adsorption of water on the silanols has been the subject of systematic studies.[44] The experimental heat of adsorption of water on silanols was measured with microcalorimetry to be between 90 and 44 kJ/mol, the latter value being close to the latent heat of water liquefaction;[44] it was concluded that silanols are hydrophilic.

H-bonded silanols in silanol nests have been suggested to be more reactive to water than isolated ones and to allow water clustering.[45,46] Many other adsorption or grafting reactions depend on the existence of several Si-OH in close vicinity. For instance, in a rather old study, Kol'tsov et al.

(11) Morrow, B. A.; McFarlan, A. J. *J. Phys. Chem.* **1992**, *96*, 1395.
(12) Vandervoort, P.; Gillisdhamers, I.; Vranken, K. C.; Vansant, E. F. *J. Chem. Soc., Faraday Trans.* **1991**, *87*, 3899.
(13) Riegel, B.; Hartmann, I.; Kiefer, W.; Gross, J.; Fricke, J. *J. Non-Cryst. Solids* **1997**, *211*, 294.
(14) Pasquarello, A.; Car, R. *Phys. Rev. Lett.* **1988**, *80*, 5145.
(15) Maciel, G. E.; Sindorf, D. W. *J. Am. Chem. Soc.* **1980**, *102*, 7606.
(16) Léonardelli, S.; Facchini, L.; Fretigny, C.; Tougne, P.; Legrand, A. P. *J. Am. Chem. Soc.* **1992**, *114*, 6412.
(17) Tuel, A.; Hommel, H.; Legrand, A. P.; Kovats, E. S. *Langmuir* **1990**, *6*, 770.
(18) Liu, C. C.; Maciel, G. E. *J. Am. Chem. Soc.* **1996**, *118*, 5103.
(19) Eckert, H.; Yesinowski, J. P.; Silver, L. A.; Stolper, E. M. *J. Phys. Chem.* **1988**, *92*, 2055.
(20) Bronnimann, C.; Zeigler, R. C.; Maciel, G. E. *J. Am. Chem. Soc.* **1988**, *110*, 2023.
(21) Chuang, I. S.; Maciel, G. E. *J. Am. Chem. Soc.* **1996**, *118*, 401.
(22) Kinney, D. R.; Chuang, I. S.; Maciel, G. E. *J. Am. Chem. Soc.* **1993**, *115*, 6786.
(23) Freude, D.; Hunger, M.; Pfeifer, H. *Chem. Phys. Lett.* **1982**, *91*, 307.
(24) Haukka, S.; Lakomaa, E. L.; Root, A. *J. Phys. Chem.* **1993**, *97*, 5085.
(25) Shantz, D. F.; auf der Gunne, J. S.; Koller, H.; Lobo, R. F. *J. Am. Chem. Soc.* **2000**, *122*, 6659.
(26) Trebosc, J.; Wiench, J. W.; Huh, S.; Lin, V. S. Y.; Pruski, M. *J. Am. Chem. Soc.* **2005**, *127*, 3057.
(27) Burneau, A.; Humbert, B.; Barres, O.; Gallas, J. P.; Lavalley, J. C. *Adv. Chem. Ser.* **1994**, *234*, 199. (Colloid Chemistry of Silica)
(28) Morrow, B. A.; McFarlan, A. J. *J. Phys. Chem.* **1992**, *96*, 1395.
(29) Kennedy, G. J.; Afeworki, M.; Calabro, D. C.; Chase, C. E.; Smiley, R. J. *Appl. Spectrosc.* **2004**, *58*, 698.
(30) Hartmeyer, G.; Marichal, C.; Lebeau, B.; Rigolet, S.; Caullet, P.; Hernandez, J. *J. Phys. Chem. C* **2007**, *111*, 9066.
(31) Shchukarev, A.; Rosenqvist, J.; Sjöberg, S. *J. Electron Spectrosc. Relat. Phenom.* **2004**, *137* (140), 171.
(32) Duval, Y.; Mielczarski, J. A.; Pokrovsky, O. S.; Mielczarski, E.; Ehrhardt, J. J. *J. Phys. Chem. B* **2002**, *106*, 2937.
(33) Chabal, Y. J.; Christman, S. B. *Phys. Rev. B* **1984**, *29*, 6974.
(34) Schroeder, T.; Giorgi, J. B.; Bäumer, M.; Freund, H. J. *Phys. Rev. B* **2002**, *66*, 165422.
(35) Schroeder, T.; Adelt, M.; Richter, B.; Naschitzki, M.; Bäumer, M.; Freund, H. J. *Surf. Rev. Lett.* **2000**, *7*, 7.
(36) Ozensoy, E.; Min, B. K.; Santra, A. K.; Goodman, D. W. *J. Phys. Chem. B* **2004**, *108*, 4351.
(37) Chen, M. S.; Santra, A. K.; Goodman, D. W. *Phys. Rev. B* **2004**, *69*, 155404.
(38) Du, M. H.; Kolchin, A.; Cheng, H. P. *J. Chem. Phys.* **2004**, *120*, 1044.
(39) Sindorf, D. W.; Maciel, G. E. *J. Phys. Chem.* **1982**, *86*, 5208.
(40) Xue, X.; Kanzaki, M. *Phys. Chem. Miner.* **1998**, *26*, 14.
(41) Boujday, S.; Lambert, J.-F.; Che, M. *ChemPhysChem* **2004**, *5*, 1003.
(42) Fisk, J. D.; Batten, R.; Jones, G.; O'Reilly, J. P.; Shaw, A. M. *J. Phys. Chem. B* **2005**, *109*, 14475.
(43) Ong, S.; Zhao, X.; Eisenthal, K. B. *Chem. Phys. Lett.* **1992**, *191*, 327.
(44) Bolis, V.; Fubini, B.; Marchese, L.; G., M.; Costa, D. *J. Chem. Soc., Faraday Trans.* **1991**, *87*, 497.
(45) Takei, T.; Chikazawa, M. J. *J. Colloid Interface Sci.* **1998**, *208*, 570.
(46) Fubini, B.; Bolis, V.; Cavengo, A.; Garrone, E.; Ugliengo, P. *Langmuir* **1993**, *9*, 2712.

proposed to use $VOCl_3$ grafting from the gas phase to quantify the number of groups of two or three neighboring silanols on an amorphous silica surface as a function of the pretreatment temperature.[47]

Because of the multiple sites exhibited on the silica surface, it might be expected that adsorbed molecules would give rise to intricate spectra, corresponding to the superposition of the responses of a variety of adsorbed species. However, some instances are known where rather sharp spectra are observed (e.g., UV spectra of $[Ni^{II}L_x(H_2O)_{6-x}]^{2+}$,[48] ^{13}C NMR of amino acids[49]) suggesting that adsorbed molecules have a strong preference to interact with specific groups.

Many theoretical studies have been performed on silica to complement the lack of information due to its amorphous nature. Different approaches have addressed different topics. On the one hand, force field calculations have allowed to propose large size models (several thousands of atoms) of vitreous/amorphous silicas, which have been compared with bulk data such as Si−O−Si angles, Si−O bond lengths, and ring size distributions.[50–55] The bulk, surfaces, and their reactivity toward water to generate a hydroxylated surface have been much less studied: after the seminal work of Feuston and Garofalini on water reactivity with a silica surface[50,51] a few works have been devoted to the water/silica interaction.[56–58] Ab initio calculations have been combined with classical MD (molecular dynamics) to obtain insight on the strength of the physisorption sites and the chemical reactivity of the anhydrous surface.[58] Only very recently a new model, generated using classical MD, for the hydroxylated amorphous silica surface has been proposed.[59] The high interest of this new model is to propose a hydroxylated surface with hydrophilic zones coexisting with hydrophobic ones.

On the other hand, first principles calculations on small size clusters (10−50 atoms) have focused on the spectroscopic properties and reactivity of the silanols with small adsorbates.[60] In particular, the interaction of water with the surface was modeled.[61–63] The adsorption of NH_3 or alcohols,[64] isobutene,[65] benzyl and phenyl containing probes,[66] metallic complexes,[67–74] and small size amino acids[49,75,76] onto the silica surface was also investigated. It is well-known that cluster studies allow the use of high accuracy quantum methods which describe energetics, reaction paths, and intermediates but might suffer from edge effect if not used in embedded techniques.

From the large size models obtained with classical methods, it is possible to extract small systems and to use them as a starting point for elaborating a new model with ab initio methods.[77–79] Alternatively, it is possible to start from molten silica models and to cool them down slowly.[80,81] Bulk amorphous silica may also be generated by cooling a preheated β-cristobalite via classical MD simulation and perform a further ab initio MD optimization.[38]

To the best of our knowledge, the models of amorphous silica surfaces used in those ab initio periodic calculations are limited to nonhydroxylated surfaces or to the study of a single defect hydroxylation. In consequence, they do not present the high silanol density of a silica surface at room temperature. In fact, no theoretical study has tried to reproduce what is empirically known of the density, nature, and distribution of surface silanols and compare predicted and observed spectroscopic properties. In this paper we report results from first-principles density functional calculations on a representative model for an amorphous hydroxylated silica surface.

Methods

Generation of the Amorphous Silica Surface. The amorphous silica surface model is inspired from the model of Garofalini[51] used in molecular mechanics calculations on pure SiO_2 glasses. Since this model is much too large to be used in periodic ab initio calculations, it was truncated to form a slab with dimensions of about 13 Å × 17.5 Å × 25 Å (of which 15 Å is vacuum) containing 26 SiO_2 units. To this structure, 13 water molecules were added as terminating OH-groups. The total number of atoms of the new

(47) Kol'tsov, S. I.; Malygin, A. A.; Volkova, A. V.; Aleskovskii, V. B. *Zh. Fiz. Khim.* **1973**, *47*, 988.
(48) Boujday, S.; Lambert, J.-F.; Che, M. *J. Phys. Chem. B* **2003**, *107*, 651.
(49) Stievano, L.; Piao, L.-Y.; Lopes, I.; Meng, M.; Cota, D.; Lambert, J.-F. *Eur. J. Miner.* **2007**, *19*, 321.
(50) Feuston, B. P.; Garofalini, S. H. *J. Appl. Phys.* **1990**, *68*, 4830.
(51) Garofalini, S. H. *Non-Cryst. Solids* **1990**, *120*, 1.
(52) Woodcock, L. V.; Angell, C. A.; Cheeseman, P. *J. Chem. Phys.* **1976**, *65*, 1565.
(53) Soules, T. F. *J. Chem. Phys.* **1979**, *71*, 4570.
(54) Mitra, S. K.; Amini, M.; Fincham, D.; Hockney, R. W. *Philos. Mag. B* **1981**, *43*, 365.
(55) Kubicki, J. D.; Lasaga, A. C. *Am. Mineral.* **1988**, *73*, 941.
(56) Bakaev, V. A.; Steele, W. A. *J. Chem. Phys.* **1999**, *111*, 9803.
(57) Leed, E. A.; Pantano, C. G. *J. Non-Cryst. Solids* **2003**, *325*, 48.
(58) Leed, E. A.; Sofo, J. O.; Pantano, C. G. *Phys. Rev. B* **2005**, *72*, 155427.
(59) Hassanali, A. A.; Singer, S. J. *J. Phys. Chem. B* **2007**, *111*, 11181.
(60) Sauer, J.; Ugliengo, P.; Garonne, E.; Saunders, V. R. *Chem. Rev* **1994**, *94*, 2095.
(61) Walsh, T. R.; Wilson, M.; Sutton, A. P. *J. Chem. Phys.* **2000**, *113*, 9191.
(62) Civalleri, B.; Garrone, E.; Ugliengo, P. *Chem. Phys. Lett.* **1999**, *299*, 443.
(63) Pelmenschikov, A. G.; Morosi, G.; Gamba, A. *J. Phys. Chem. A* **1997**, *101*, 1178.
(64) Natal-Santiago, M. A.; Dumesic, J. A. *J. Catal.* **1998**, *175*, 252.
(65) Natal-Santiago, M. A.; dePablo, J. J.; Dumesic, J. A. *Catal. Lett.* **1997**, *47*, 119.
(66) Granqvist, B.; Sandberg, T.; Hotokka, M. *J. Colloid Interface Sci.* **2007**, *310*, 369.
(67) Pietrzyk, P. *J. Phys. Chem. B* **2005**, *108*, 10291.
(68) Lopez, N.; Illas, F.; Pacchioni, G. *J. Phys. Chem. B* **1999**, *103*, 8552.
(69) Costa, D.; Martra, G.; Che, M.; Manceron, L.; Kermarec, M. *J. Am. Chem. Soc.* **2002**, *124*, 7210.
(70) Martra, G.; S., C.; Che, M.; Manceron, L.; Kermarec, M.; Costa, D. *J. Phys. Chem. B* **2003**, *107*, 6096.
(71) Bromley, S. T.; Sankar, G.; Catlow, C. R. A.; Maschmeyer, T.; Johnson, B. F. G.; Thomas, J. M. *Chem. Phys. Lett.* **2001**, *340*, 524.
(72) Ustynyuk, L. Y.; Ustynyuk, Y. A.; Laikov, D. N.; Lunin, V. V. *Russ. Chem. Bull.* **2001**, *50*, 2050.
(73) Tada, M.; Sasaki, T.; Shido, T.; Iwasawa, Y. *Phys. Chem. Chem. Phys.* **2002**, *4*, 5899.
(74) Tada, M.; Sasaki, T.; Iwasawa, Y. *J. Phys. Chem. B* **2004**, *108*, 2918.
(75) Costa, D.; Lomenech, C.; Meng, M.; Stievano, L.; Lambert, J.-F. *J. Mol. Struct. (Theochem)* **2007**, *806*, 253.
(76) Lomenech, C.; Bery, G.; Costa, D.; Stievano, L.; Lambert, J.-F. *PhysChemPhys* **2005**, *6*, 1061.
(77) Benoit, M.; Ispas, S.; Tuckerman, M. E. *Phys. Rev. B* **2001**, *64*, 224205.
(78) Ceresoli, D.; Bernasconi, M.; Iarlori, S.; Parrinello, M.; Tosatti, E. *Phys. Rev. Lett.* **2000**, *84*, 3787.
(79) Masini, P.; Bernasconi, M. *J. Phys.: Condens. Matter* **2002**, *14*, 4133.
(80) Sarnthein, J.; Pasquarello, A.; Car, R. *Phys. Rev. B* **1995**, *52*, 12690.
(81) Van Ginhoven, R. M.; Jonsson, H.; Corrales, L. R. *Phys. Rev. B* **2005**, *71*, 024208.

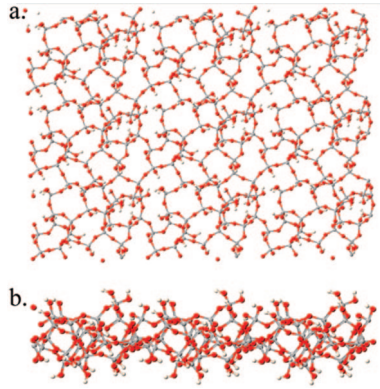

Figure 1. Picture showing the top view (a) and side view (b) of the model silica surface.

hydrated slab is 120 ($Si_{26}O_{65}H_{27}$). The slab has a density of approximately 1.7 g/cm^3. The number of Si atoms belonging to tetrahedra exposed on the surface is approximately 8/nm^2.

The atom positions and cell dimensions were relaxed using ab initio MD at constant temperature (400 K). The time step was set at 3 fs, and the geometries were sampled up to 5 ps to have a reliable image of the equilibrium geometry at 400 K using a microcanonical ensemble. Higher temperatures show dehydroxylation and ring closing, making the surface less hydrophilic, which is in agreement with experimental observations.[82] In a second step the equilibrated slab was completely (i.e., without geometrical constraints) optimized at 0 K. Because of the large cell size, the Γ-point was used for the Brillouin zone integration and a plane-wave energy cutoff of 230 eV, followed by an optimization performed at a 3 × 2 × 1 *k*-point mesh for the Brillouin-zone integration with an energy cutoff of 400 eV. After the geometry optimization the obtained surface was 12.8 Å long × 17.6 Å wide with a slab thickness varying from 5.2 Å to 8.2 Å, corresponding to a three-layer slab (see Figure 1a). The obtained surface is described in the first part of the Results and Discussion section.

The geometry optimization and minimization of the total energy were performed using the VASP code.[83,84] In the periodic density functional theory framework used, the Kohn−Sham equations have been solved by means of the Perdew−Burke−Ernzerhof (PBE) functional.[85–88] The electron−ion interaction was described by the projector augmented-wave (PAW) method.[89,90]

The gas phase acidity of the hydroxyls was evaluated using the deprotonation energy ΔE, for the reaction $AH \rightarrow A^- + H^+$. The ΔE was calculated as the difference between the energy of the optimized protonated structure and the energy of the optimized conjugated base. An increase in deprotonation energy indicated a decrease in acidity.

To calculate the Hessian matrix, finite differences are used; that is, each ion is displaced in the direction of each Cartesian coordinate, and the Hessian matrix is determined from the forces. All atoms are displaced in all three Cartesian directions. The frequency calculations were performed considering one *k*-point.

The first principles NMR calculations were performed within Kohn−Sham DFT using the PARATEC code.[91] The PBE generalized gradient approximation[85–88] was used, and the valence electrons were described by norm conserving pseudopotentials[92] in the Kleinman−Bylander[93] form. The core definition for O is $1s^2$ and $1s^22s^22p^6$ for Si. The core radii are 1.2 au for H, 1.5 au for O, and 2.0 au for Si. The wave functions are expanded on a plane wave basis set with a kinetic energy cutoff of 1088 eV.

The integral over the first Brillouin zone is performed using a Monkhorst-Pack 2 × 2 × 1 *k*-point grid[94] for the charge density and chemical shift tensor calculation. The shielding tensor is computed using the GIPAW[95] approach which permits the reproduction of the results of a fully converged all-electron calculation. The isotropic chemical shift δ_{iso} is defined as $\delta_{iso} = -[\sigma - \sigma^{ref}]$ where σ is the isotropic shielding and σ^{ref} is the isotropic shielding of the same nucleus in a reference system as previously described.[96,97]

The calculations have been performed at the IDRIS supercomputer center of the CNRS using a parallel IBM Power4 (1.3 GHz) computer.

Results and Discussion

Geometry of the Amorphous Silica Surface. The slab is formed by a superposition of interconnected irregular $(SiO_2)_n$ ring structures of various sizes. The resulting surface contains principally four, five, and six-membered rings. There are also some larger rings (from 7 to 10 tetrahedra). In our model slab the distribution is 4:3:4:1:1:1 and 1 for the 4, 5, 6, 7, 8, 9, and 10-membered rings, respectively. Smaller rings (two and three rings) were absent, as intuitively expected since they are more strained and rigid, and are known to open after hydration of the surface.

The Si−O distance analysis shows the distribution being centered on 1.66 Å (ranging from 1.64 Å to 1.72 Å). The value of 1.66 Å is in very good agreement with the high level calculations on the disiloxane molecule.[98] The average Si−O bond length in amorphous silica has been reported to be 1.62 Å.[99]

The Si−O−Si angles range from 130° to almost 180° (see Figure 2), having a maximum around 142−150°. Small values for the Si−O−Si angle generally correspond to small rings. However, it was shown by Athanasopoulos and Garofalini[100] that the decrease in Si−O−Si angle is not directly related to the presence of small rings but rather to the deformation of five- and six-membered rings. Indeed, since no strongly strained two- or three-membered rings are present in our model, the mean value agrees with the

(82) D'Souza, A. S.; Pantano, C. G. *J. Am. Ceram. Soc.* **1999**, *28*, 1289.
(83) Kresse, G.; Hafner, J. *Phys. Rev. B* **1994**, *49*, 14251.
(84) Kresse, G.; Furthmuller, J. *Comput. Mater. Sci.* **1996**, *6*, 15.
(85) Perdew, J. P.; Burke, K.; Ernzerhof, M. *Phys. Rev. Lett.* **1996**, *77*, 3865.
(86) Perdew, J. P.; Burke, K.; Ernzerhof, M. *Phys. Rev. Lett.* **1997**, *78*, 1396.
(87) Zhang, Y. K.; Yang, W. T. *Phys. Rev. Lett.* **1998**, *80*, 890.
(88) Perdew, J. P.; Burke, K.; M., E. *Phys. Rev. Lett.* **1996**, *77*, 3865.
(89) Blöchl, P. E.; Jepsen, O.; Andersen, O. K. *Phys. Rev. B* **1994**, *49*, 16223.
(90) Kresse, G.; Joubert, D. *Phys. Rev. B* **1999**, *59*, 1758.
(91) Mauri, F.; Cote, M.; Yoon, Y.; Pickard, C.; Heynes, P. *PARATEC (PARAllel Total Energy Code)*; Pfrommer, B., Raczkowski, D., Canning, A., Louie, S. G., Eds.; Lawrence Berkeley National Laboratory, www.nersc.gov/projects/paratec.
(92) Troullier, N.; Martins, J. L. *Phys. Rev. B* **1991**, *43*, 1993.
(93) Kleinman, L.; Bylander, D. *Phys. Rev. Lett.* **1982**, *48*, 1425.
(94) Monkhorst, H. J.; Pack, J. D. *Phys. Rev. B* **1976**, *13*, 5188.
(95) Pickard, C. J.; Mauri, F. *Phys. Rev. B* **2001**, *63*, 245101.
(96) Gervais, C.; Profeta, M.; Lafond, V.; Bonhomme, C.; Azaïs, T.; Mutin, H.; Pickard, C. J.; Mauri, F.; Babonneau, F. *Magn. Reson. Chem.* **2004**, *42*, 445.
(97) Gervais, C.; Dupree, R.; Pike, K.; Bonhomme, C.; Profeta, M.; Pickard, C. J.; Mauri, F. *J. Phys. Chem. A* **2005**, *109*, 6960.
(98) Tielens, F.; De Proft, F.; Geerlings, P. *J. Mol. Struct. (Theochem)* **2001**, *542*, 227.
(99) Mozzi, R. L.; Warren, B. E. *J. Appl. Crystallogr.* **1969**, *2*, 164.
(100) Athanasopoulos, D. C.; Garofalini, S. H. *J. Chem. Phys.* **1992**, *97*, 3775.

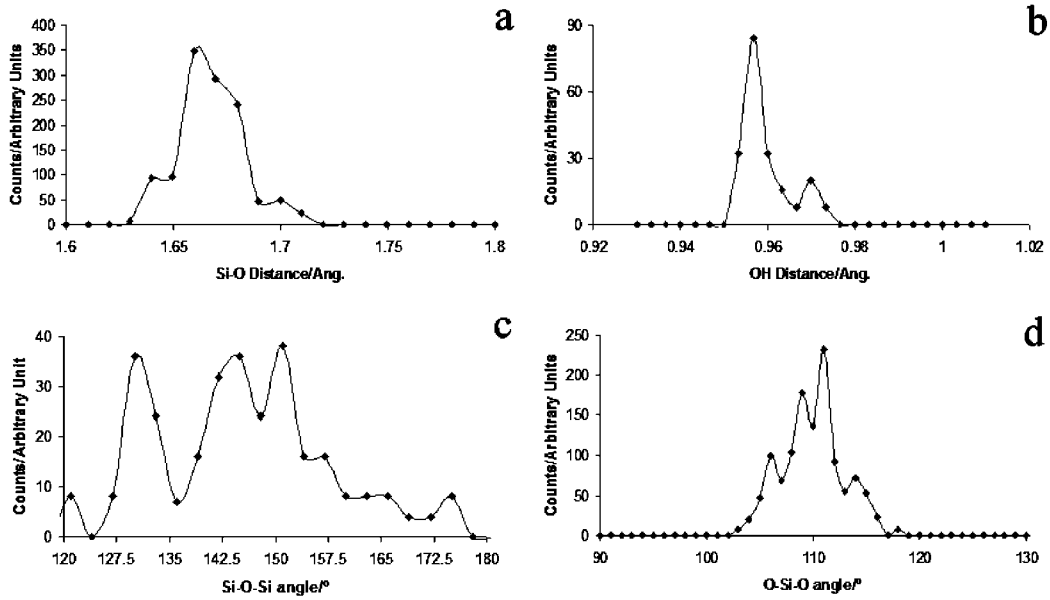

Figure 2. a. Si−O bond distance distribution in the model slab. b. O−H bond distance distribution in the model slab. c. Si−O−Si angle distribution in the model slab. d. O−Si−O angle distribution in the model slab.

Table 1. Overview of the Different Number/Nature of Silanols on the Slab Compared with Experiment

density and nature of the silanols on the two faces of the slab	top surface	bottom surface	experimental value
silanols density (OH/nm^2)	5.8	5.8	4.9
geminal/(geminal + terminal) ratio	0.23	0.46	0.1−0.3
vicinal/(vicinal + adjacent) total ratio	0.92	1	not reported
silanols involved in H bonds	0.38	0.31	not reported

presence of deformed five- and six-membered rings. It is also known that the Si−O−Si angle has a very low bending barrier (the barrier to linearity is only 1.80 kJ/mol),[98] which is confirmed by the broad distribution of this parameter as can be seen in Figure 2.

The distribution of the O−Si−O angle (see Figure 2) shows a maximum around 111° (very close to the tetrahedral angle). This distribution is in agreement with observations in α-quartz where a small shift to higher values is noticed as well.

The correct description of the Si−O−Si angle is very important as it provides an extremely useful test for theoretical calculation methods. The geometrical parameters may be directly compared with high level DFT results obtained for the elementary building block of silicas, silanol, and disiloxane, studied by one of us in the past.[98] In contrast, the distribution of the O−Si−O angles is much narrower, in agreement with the intuitive idea that the structure of silica polymorphs is made of rigid (SiO_4) tetrahedra connected by Si−O−Si hinges.

As outlined in the Introduction part, the main purpose of the present paper is to propose a model of amorphous silica taking into account the density, nature of silanols, and H bond network present on a real amorphous surface, as those silanols are responsible for silica reactivity. Table 1 summarizes the characteristics of our model concerning those SiOH groups: two opposite surfaces were created when generating the slab. We refer to them (arbitrarily) as top and bottom surfaces, as shown in Figure 1. The concentration of surface hydroxyls is 5.8/nm^2 on each surface, which is quite close to the experimental estimates on a hydroxylated surface (see discussion in the Introduction). On the top surface, 23% silanols are geminal ones, in good agreement with experimental values; in contrast, the bottom surface presents a higher geminal density. Most of the silanols are vicinal ones, due to the relatively high silanol surface density. Only one silanol is surrounded by Q_4 Si atoms (Si atoms bearing no OH group), but even in this case it has adjacent silanols in the neighborhood. Finally, 38% (respectively at the bottom surface 31%) of the silanols are involved in H bonds. To summarize, the slab proposed here exhibits a silanol density and distribution (geminal/terminal proportion) compatible with experiment; the large majority of silanols are vicinal ones, from which one-third are H bonded whereas 2/3 remain isolated. A summary of the different types of silanols on our model surface compared with experiment is shown in Table 1.

NMR Analysis. Various ab initio calculations have been carried out previously[40,101−107] on silicate clusters to determine possible correlations between local structure and NMR parameters, with special attention to ^{17}O NMR. These results have been compared to experimental ones to translate a distribution of ^{17}O quadrupolar parameters into a distribution of structural parameters such as the Si−O−Si angles and Si−O distances.[108,109] Alternative approaches involve the use of periodic boundary conditions: Pickard and Mauri[110] introduced a plane wave pseudopotential method for calculating NMR parameters. Their calculated values for a variety

(101) Casanovas, J.; Pacchioni, G.; Illas, F. *Mater. Sci. Eng.* **1999**, *68*, 16.
(102) Tossell, J. A.; Lazzeretti, P. *Chem. Phys.* **1987**, *112*, 205.
(103) Tossell, J. A.; Lazzeretti, P. *Phys. Chem. Miner.* **1988**, *15*, 564.
(104) Lindsay, C. G.; Tossell, J. A. *Phys. Chem. Miner.* **1991**, *18*, 191.
(105) Clark, T. M.; Grandinetti, P. J. *Solid State Nucl. Magn. Reson.* **2000**, *16*, 55.
(106) Xue, X.; Kanzaki, M. *Solid State Nucl. Magn. Reson.* **2000**, *16*, 245.
(107) Xue, X.; Kanzaki, M. *J. Phys. Chem. B* **2001**, *205*, 3422.
(108) Farnan, I.; Grandinetti, P. J.; Baltisberger, J. H.; Stebbins, J. F.; Werner, U.; Eastman, M. A.; Pines, A. *Nature* **1992**, *358*, 31.
(109) Clark, T. M.; Grandinetti, P. J. *J. Phys.: Condens. Matter* **2003**, *15*, 2387.

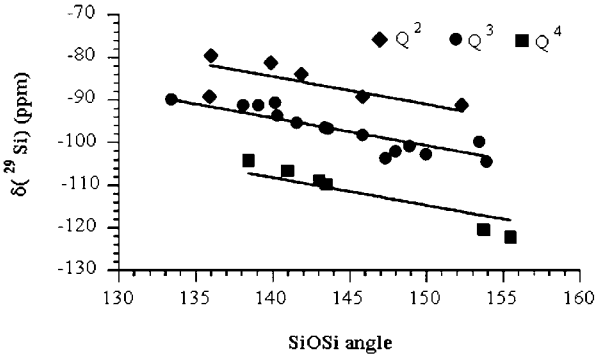

Figure 3. Calculated ^{29}Si isotropic chemical shift values as a function of the mean Si−O−Si angle for the Q^2, Q^3, and Q^4 sites of the silica surface. Solid lines represent the fits obtained with eq 1 proposed in refs 117 and 118.

of silica polymorphs were shown to be in excellent agreement with experimental data.[111]

The relevance of our amorphous silica surface model was checked by comparing the calculated NMR parameters (using the periodic approach) with experimental values concerning Si−O−Si bonds in similar systems. The obtained results were also confronted with the relationships previously proposed between NMR properties and local environments. Obviously, it would be particularly important to understand the ^{1}H and ^{17}O NMR characteristics of the atoms included in silanol groups since the latter determine the adsorptive behavior. It would for instance be interesting to establish correlations between the NMR parameters and the hydrogen bonding state of silanols. So far, however, very few experimental ^{17}O NMR data[112,113] have been reported for Si-OH groups.

^{29}Si NMR. The ^{29}Si isotropic chemical shifts calculated for our model are in the −104.1 to −122.1 ppm range for Q^4 ($Si(OSi)_4$), −89.2 to −104.3 ppm for Q^3 ($Si(OSi)_3OH$), and −79.6 to −91.2 ppm for Q^2 ($Si(OSi)_2(OH)_2$), in good agreement with reported experimental values in silicate minerals[114] silicate solutions,[115] silica gels[18,116] and precipitated silica.[16] The chemical shift values of Q^2, Q^3, and Q^4 decrease linearly with increasing mean Si−O−Si angles for each silicon site (see Figure 3) consistently with experimental data: linear correlations between $^{29}Si(\delta_{iso})$ and several functions of the Si−O−Si angle α have been suggested.[115] The simplest correlation equation proposed is

$$^{29}\mathrm{Si}(\delta_{iso}) = a + b\alpha \quad (1)$$

with $a = -25.44$[117] or −18.68 ppm[118] and $b = -0.5793$[117] or −0.6192 ppm[118] for Q^4 sites in zeolites and silica polymorphs. By fitting the ab initio calculated $^{29}Si(\delta_{iso})$ with eq 1, we obtain the correlation shown as the solid curves in Figure 3 with $b = -0.65$ for all type of sites and $a = -17.1$, −3.1, and +6.5 ppm for Q^4, Q^3, and Q^2 sites, respectively.

^{17}O NMR. The calculated ^{17}O isotropic chemical shifts for bridging oxygens in Si−O−Si environments are in the 40.2−75.7 ppm range, which is in good agreement with the values reported in silicate minerals[114] and silica polymorphs.[111,119–121] In view of the established correlation between ^{29}Si chemical shifts and Si−O−Si angle, it is tempting to look for a similar correlation of the ^{17}O chemical shifts, but no clear evidence has been found yet. Our data (Figure 4a) show a decrease of $\delta_{iso}(^{17}O)$ with increasing Si−O−Si angle which is consistent with values reported for silica polymorphs,[111] but even if a general trend is visible, it is clear that $\delta_{iso}(^{17}O)$ is not a simple function of the Si−O−Si angle. A dependence of the ^{17}O quadrupolar coupling parameters of bridging oxygen on Si−O distances and Si−O−Si angles has been suggested.[103,108,109] The quadrupolar interaction can indeed be characterized by the quadrupolar coupling constant C_Q and the asymmetry parameter η_Q defined as

$$C_Q = eQV_{zz}/h \quad \text{and} \quad \eta_Q = (V_{yy} - V_{xx})/V_{zz} \quad (2)$$

where V_{xx}, V_{yy}, and V_{zz} are the principal components of the EFG (electric field gradient) tensor defined as $|V_{zz}| \geq |V_{xx}| \geq |V_{yy}|$ and Q is the ^{17}O nuclear quadrupole moment.

Regarding the ^{17}O quadrupolar coupling constant, the following relation between C_Q and both average Si−O distance (d) and Si−O−Si angle (α) has been proposed recently:[105]

$$C_Q = a\{0.5 + [\cos\alpha/(\cos\alpha - 1)]\}^b + m(d - d^0) \quad (3)$$

where $a = -6.53$ MHz, $b = 1.80$, $m = -12.86$ MHz Å^{-1}, and $d^0 = 1.654$ Å. Since the Si−O distances distribution for our model of the amorphous silica surface shows a maximum at 1.66 Å with a global range between 1.64 and 1.72 Å, these three d values were used to fit the calculated data (Figure 4b). It appears that the fit with d = 1.66 Å is in good agreement with a majority of the points while the fits with d = 1.64 and 1.72 Å delimit the global distribution of data points. Concerning the ^{17}O asymmetry parameter η_Q, it is reported to be independent of Si−O distance and its behavior is dominated by its

(110) Pickard, C. J.; Mauri, F. In *Calculation of NMR and EPR Parameters: Theory and Applications*; Knaupp, M., Ed; Wiley-VCH: Weinheim, 2004.
(111) Profeta, M.; Mauri, F.; Pickard, C. J. *J. Am. Chem. Soc.* **2003**, *125*, 541.
(112) Cong, X.; Kirkpatrick, R. J. *J. Am. Ceram. Soc.* **1996**, *79*, 1585.
(113) van Eck, E. R. H.; Smith, M. E.; Kohn, S. C. *Solid State Nucl. Magn. Reson.* **1999**, *15*, 181.
(114) Stebbins, J. F. In *Mineral Physics and Crystallography, a Handbook of Phyisical Constants*; Ahrens, T. J., Ed.; American Geographical Union: Washington, DC, 1995; p 303.
(115) Engelhardt, G.; Koller, H. In *NMR Basic Principles and Progress*; Diehl, P., Fluck, E., Gunther, H., Kosfeld, R., Seeing, J., Eds.; Springer Verlag: Berlin, 1994; Vol. 33, p 30.
(116) Vega, A. J.; Scherer, G. W. *J. Non-Cryst. Solids* **1989**, *111*, 153.
(117) Thomas, J. M.; Klinowski, J.; Ramdas, S.; Hunter, B. K.; Tennakoom, D. T. B. *Chem. Phys. Lett.* **1983**, *102*, 18.
(118) Engelhardt, G.; Radeglia, R. *Chem. Phys. Lett.* **1984**, *108*, 271.
(119) Grandinetti, P. J.; Baltisberger, J. H.; Farnan, I.; Stebbins, J. F.; Werner, U.; Pines, A. *J. Phys. Chem.* **1995**, *99*, 12341.
(120) Bull, L. M.; Bussemer, B.; Anupold, T.; Reinold, A.; Samoson, A.; Sauer, J.; Cheetham, A. K.; Dupree, R. *J. Am. Chem. Soc.* **2000**, *122*, 4948.
(121) Bull, L. M.; Cheetham, A. K.; Anupold, T.; Reinold, A.; Samoson, A.; Sauer, J.; Bussemer, B.; Lee, Y.; Gann, S.; Shore, J.; Pines, A. *J. Am. Chem. Soc.* **1998**, *120*, 3510.

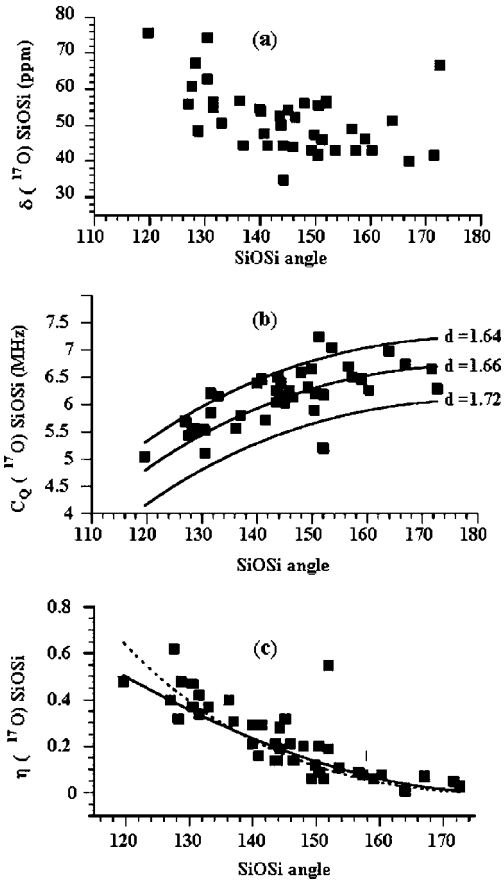

Figure 4. (a) Calculated ^{17}O isotropic chemical shifts, (b) calculated quadrupolar coupling constants C_Q, and (c) calculated asymmetry parameter η of bridging oxygens Si−O−Si as a function of Si−O−Si angle C_Q values (b) are fitted with eq 2 from ref 105 with $d = 1.64$, 1.66, and 1.72 Å. η values (c) are fitted with eq (3) from ref 103 (solid line) and eq (4) from ref105 (dashed line).

dependence on Si−O−Si angle. Various correlations have been proposed: the ab initio based empirical relationship[103]

$$\eta_Q = 1 + \cos\alpha \tag{4}$$

has been used[108] to investigate the Si−O−Si angle distribution in silicate glasses; the modified semiempirical correlation

$$\eta = a'\{0.5 - [\cos\alpha/(\cos\alpha - 1)]\}^{b'} \tag{5}$$

has been proposed to fit the experimental values of silica polymorphs[105] with $a' = 4.73$ and $b' = 1.12$. Both equations were used to fit our data, and a satisfying agreement is observed (Figure 4c).

The calculated ^{17}O isotropic chemical shifts for silanol oxygens Si−O−H range from −9.8 to 36.9 ppm consistently with solution NMR data on silica gels precursors[122] and solid-state NMR studies on silica gels[112,113] and talc ($Mg_3Si_4O_{10}(OH)_2$).[123] There is no clear dependence of $\delta_{iso}(^{17}O)$ with the hydrogen-bonding strength or any other simple structural parameter.[40,107] On the contrary, a tendency is observed for ^{17}O quadrupolar coupling constant values: they lie in the 6.4−8.1 MHz range and decrease with increasing O−H bond length (Figure 5). This tendency and the observed range are consistent with previous calculations.[40,107] It should be noticed that the calculated C_Q values are significantly higher than those experimentally determined in silica gels[112,113,123] (around 4 MHz). This was tentatively explained either by a preferential ^{17}O NMR detection of the SiOH sites with strong hydrogen bonding or by a significant motional narrowing.[107]

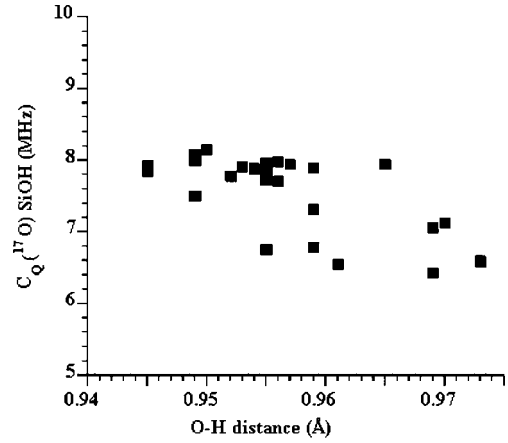

Figure 5. Calculated ^{17}O quadrupolar coupling constants C_Q of silanol sites Si−O−H as a function of O−H bond length.

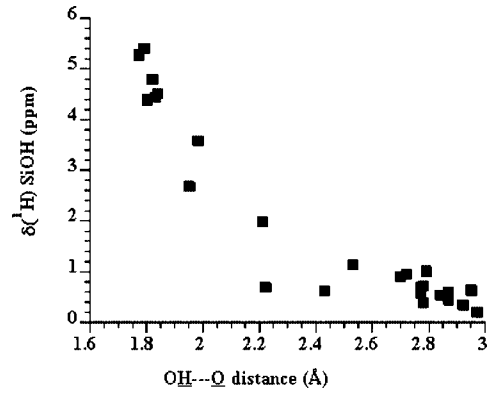

Figure 6. Calculated ^1H isotropic chemical shift values of silanol sites Si−O−H as a function of OH···O distances

^1H NMR. The calculated proton chemical shift range is quite large (ranging from 0.2 to 5.4 ppm), which is in good agreement with experimental values for silicate glasses[19] fumed silica[18] and silica gels.[20–23]

Hydrogen bonding interactions may be responsible for this large range of calculated chemical shifts. When comparing the shortest $d_{OH\cdots O}$ (distances between the italicized atoms) with the calculated chemical shift for all silanol sites, strong variations are observed for $d_{OH\cdots O}$, ranging from 1.7 to 3.0 Å. As a matter of fact, $\delta_{iso}(^1H)$ decreases for longer $d_{OH\cdots O}$ hydrogen bond lengths (Figure 6), as already reported from previous calculations in silicate clusters[40,107] and from experimental NMR data on organic and inorganic compounds.[124–126] It can be noticed that the contribution from hydrogen bonds seems to become relatively small at long $d_{OH\cdots O}$ distances considering the much smaller slope observed in Figure 6 for $d_{OH\cdots O} > 2.2$ Å.

(122) Delattre, L.; Babonneau, F. *Chem. Mater.* **1997**, *9*, 2385.
(123) Walter, T. H.; Turner, G. L.; Oldfield, E. *J. Magn. Reson.* **1988**, *76*, 106.
(124) Berglund, R. W. V. *J. Chem. Phys.* **1980**, *73*, 2037.
(125) Jeffrey, A.; Yeon, Y. *Acta Crystallogr., Sect. B* **1986**, *42*, 410.
(126) Gervais, C.; Coelho, C.; Azaïs, T.; Maquet, J.; Laurent, G.; Pourpoint, F.; Bonhomme, C.; Florian, P.; Alonso, B.; Guerrero, G.; Mutin, P. H.; Mauri, F. *J. Magn. Reson.* **2007**, *187*, 131.

Acidity of the Surface Hydroxyls. Acidity can be analyzed with theoretical tools by the study of such intrinsic properties as charge, LUMO levels, and especially in the case of Brønsted acids, deprotonation energies and OH vibrational frequencies, whereas the ranking obtained by probe molecule adsorption is extrinsic. In this study we examined the deprotonation energies and OH vibrational frequencies.

Deprotonation Energies. Relative gas-phase acidities are readily estimated from surface models. The gas phase deprotonation of a surface group can be written as

$$\text{X-OH} = \text{X-O}^- + \text{H}^+ \quad (6)$$

and the more acidic surface groups will correspond to the less positive energy changes in the above reaction; if we want to predict relative acidities, they will follow the relative deprotonation energies:

$$\Delta E = E(\text{X-O}^-) - E(\text{X-OH}) \quad (7)$$

Most experimental data are concerned with acidities in the presence of an aqueous phase (e.g., in silica suspensions), and the hydration energies of both the protonated and the deprotonated species should be taken into account to evaluate them. In principle, the tendencies could therefore be different in the gas phase and in the aqueous phase; in fact, it has been reported that surface OH deprotonation energies (ΔE) are a good predictor of acidity constants in solution.[127,128] The more positive the deprotonation energy, the less acidic the OH group will be toward a solution.

The acidity of silanol groups depends on geometric features: more precisely, acidities are directly related to the Si−O−Si angles.[60,129] Most probably, it is also controlled by the existence of other surface groups in the vicinity.

In our model, the vicinal hydroxyl groups are found to have a deprotonation energy of about 650 kJ/mol and the geminal ones of about 600 kJ/mol: thus, geminal silanols should be slightly more acidic than vicinal ones. The difference between both types of silanols is only about 50 kJ/mol, and one may wonder if this difference is enough to confidently predict the order of acidity in the presence of an aqueous phase. The $\Delta E/\text{p}K_\text{a}$ correlation proposed by Tossell and Sahai[128] leads one to expect the $\text{p}K_\text{a}$ of geminal silanols to be inferior to that of vicinal silanols by 2.6 pK units. While this value probably still lies within the uncertainty limit, such calculations are certainly relevant when assigning $\text{p}K_\text{a}$ values to specific surface groups.

OH Frequency Calculations. The harmonic vibrational frequencies of the surface hydroxyl groups are reported in Figure 7 as a function of the O−H bond length. It should be noted that one might expect anharmonic contributions in the experimental values. Nevertheless, a linear relationship was obtained between the OH bond length and the calculated frequency. Two linear regression curves were plotted, one from the data obtained on geminal silanols and the other one from data obtained on terminal silanols. Both curves

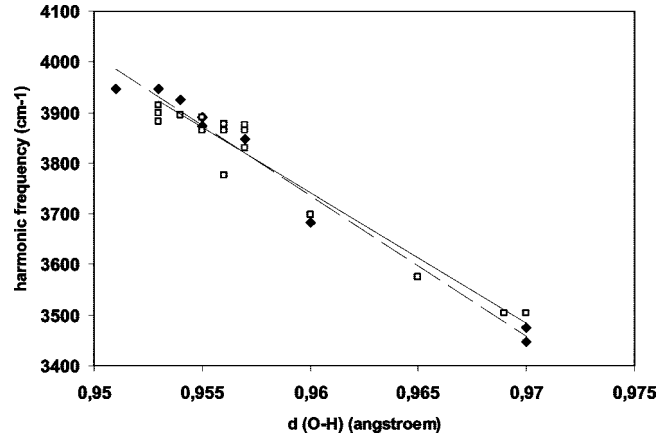

Figure 7. Calculated OH harmonic vibration frequencies (cm^{-1}) as a function of the OH bond length (Å). (◆) geminal silanols; (□) terminal silanols.

are quite similar, which suggests that the terminal or geminal nature of the silanol does not significantly influence the OH stretch frequency. However, going deeper into the analysis, we note that the calculated frequencies may be divided in three domains: the highest frequencies of vibration (3947 cm^{-1}) correspond to geminal silanols, either free or H bond acceptors. A larger domain lies between 3925 and 3831 cm^{-1} and corresponds to unbounded or H bond acceptor vicinal silanols. Then, we observe a broad domain from 3775 to 3447 cm^{-1} corresponding to H donor silanols, either terminal or geminal ones. We note also that the two geminal silanols in a pair do not vibrate at the same frequency. In many cases this can be explained by differences in the H bonding patterns in which each silanol is involved, but also in the case of a pair of nonassociated geminal silanols, we observe a significant difference of 36 cm^{-1} between the frequencies of those silanols.

Our model thus reproduces the main experimental observation of (i) a sharp band due to unbounded and H bond acceptor silanols and (ii) a large band due to silanols involved in H bond donor interaction.

Additionally, the results suggest that this sharp band could be split in two components: the upper domain could be due to vibrations of free or H bond acceptor geminal silanols, followed in the lower part of the high frequencies by vibrations of free or H bond acceptor vicinal silanols.

Adsorption of Water on Silanols. Water can be adsorbed onto the surface silanols via hydrogen bonds with an adsorption energy higher than 44 kJ/mol (which is the latent heat of liquefaction of water).[44] This result identifies the silica surface as hydrophilic. The interaction of a single water molecule was studied with a pair of geminal silanols and an isolated terminal silanol (Figure 8). It was found that the energy of interaction varies only slightly with the nature of the adsorption site, with an adsorption energy between 46 and 50 kJ/mol, slightly higher (4 kJ/mol) with the geminal than with the isolated silanol. In the latter case, two configurations were investigated, one with the water H bonded to one silanol only (Figure 8b) and one with water H-bonded to the silanol and a bridging O (Figure 8c).

Very similar heats of adsorption (51 kJ/mol) were obtained by other theoretical works for water on vicinal silanols.[38]

(127) Murashov, V. *J. Mol. Struct. (Theochem)* **2003**, *650*, 141.
(128) Tossell, J. A.; Sahai, N. *Geochim. Cosmochim. Acta* **2000**, *64*, 4097.
(129) Tielens, F.; Langenaeker, W.; Geerlings, P. *J. Mol. Struct. (Theochem)* **2000**, *496*, 153.

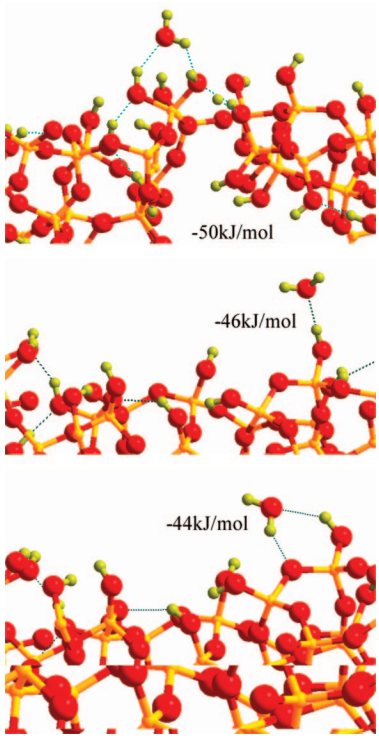

Figure 8. Interaction of a single water molecule with a pair of geminal silanols and an isolated terminal silanol in interaction with and without a lattice oxygen.

A slightly higher heat of adsorption of water on geminal (46.5 kJ/mol) than on isolated silanols (37.5 kJ/mol) has been calculated by Ugliengo et al.[62] Other works conclude on an identical heat of adsorption of water of 38 and 39 kJ/mol on the isolated and geminal silanols, respectively.[63]

Conclusions

Our new model for the hydroxylated surface of amorphous silica reproduces quite well the overall density of silanol groups and their distribution between the two main types—geminal and terminal—as observed on divided silicas; it also presents a broad range of H-bonding interactions with varying strengths and may therefore be considered as a representative model of the divided hydroxylated SiO_2 surface. Of course we do not claim with the present model to cover all the possible configurations of "real life" hydroxylated amorphous surfaces but rather to propose one possible configuration, representative in terms of ring size, silanol nature, and distribution, of an amorphous surface. Those parameters indeed determine the silica reactivity. Other geometrical features that appear to be quite reasonable are the ranges of O−Si−O and Si−O−Si angles,and Si−O bond lengths.

To check the relevance of this model for the rationalization of experimental results, spectroscopic properties such as NMR parameters and OH vibrational frequencies and properties related to reactivity such as deprotonation energies and the adsorption energy of water molecules have been investigated. The results have been compared with former theoretical data and with experimental results.

The calculation of NMR parameters (chemical shift and, for ^{17}O, quadrupolar coupling parameters) shows good agreement with experimental values reported for silicate minerals, silicate solutions, silica gels, and precipitated silicas. Moreover, such calculations allow insight into the possible correlations between NMR properties and local structures of the silica surface such as the hydrogen-bonding network to be gained.

The geminal silanols are slightly more acidic than the vicinal silanols, which has bearing on the assignment of pK_a values in aqueous suspensions.

An interaction energy of about 50 $kJ \cdot mol^{-1}$ is found for water molecules interacting with the surface through the geminal silanols, in good agreement with former model calculations and calorimetric experiments.

This new representative model for the complex amorphous hydrated silica surface, characterized at a high calculation level, should be very helpful in the investigation of its chemical reactivity, for example, to check water clustering on hydrophilic surface patches and to study the adsorption of amino acids or other organic molecules, as well as the deposition of transition metal catalyst precursors. The modeling of prebiotic chemistry and industrial catalytic reactions are only a few examples of the next possible steps.

Acknowledgment. The computation facilities provided by IDRIS and by CCRE (Université Pierre et Marie Curie) are acknowledged. Dr. B. Diawara is acknowledged for providing the molecular visualization tool ModelView.

Supporting Information Available: The calculated ^{1}H, ^{29}Si, and ^{17}O NMR parameters as well as corresponding Si−O−Si angles and $OH\cdots O$ distances (PDF). This material is available free of charge via the Internet at http://pubs.acs.org.

CM8001173